

References

- AUTHIER, A. (1968). *Phys. Status Solidi*, **27**, 77–93.
- BEDYŃSKA, T., BUBÁKOVÁ, R. & ŠOUREK, M. (1976). *Phys. Status Solidi A*, **36**, 509–516.
- BUBÁKOVÁ, R. & ŠOUREK, M. (1976). *Phys. Status Solidi A*, **35**, 55–64.
- BURNS, R. C., ROBERTSON, S. H. & KEDDY, R. J. (1993). In *The Physical Properties of Natural and Synthetic Diamonds*, edited by J. E. FIELD. New York: Academic Press.
- GRONKOWSKI, J. (1980). *Phys. Status Solidi A*, **57**, 105–112.
- GRONKOWSKI, J. & MALGRANGE, C. (1984). *Acta Cryst.* **A40**, 515–522.
- JIANG, S.-S. & LANG, A. R. (1983). *Proc. R. Soc. London Ser. A*, **388**, 249–271.
- KATO, N. (1974). *X-ray Diffraction*, by L. V. AZÁROFF, R. KAPLOW, N. KATO, R. J. WEISS, A. J. C. WILSON & R. A. YOUNG, chs. 3–5, pp. 176–438. New York: McGraw-Hill.
- KATO, N., USAMI, K. & KATAGAWA, T. (1967). *Adv. X-ray Anal.* **10**, 46–66.
- KOWALSKI, G. & LANG, A. R. (1986). *J. Appl. Cryst.* **19**, 224–228.
- KOWALSKI, G., LANG, A. R., MAKEPEACE, A. P. W. & MOORE, M. (1989). *J. Appl. Cryst.* **22**, 410–430.
- STRONG, H. M. & WENTORF, R. H. JR (1972). *Naturwissenschaften*, **59**, 1–7.
- WIERZCHOWSKI, W. & MOORE, M. (1992). *Acta Phys. Pol.* **82**, 185–191.
- WIERZCHOWSKI, W., MOORE, M., MAKEPEACE, A. P. W. & YACOOT, A. (1991). *J. Cryst. Growth*, **114**, 209–227.

Acta Cryst. (1995). **A51**, 840–845

A Tangent Formula Derived from Patterson-Function Arguments. III. Structure Determination of Zeolitic and Layered Materials from Low-Resolution Powder Diffraction Data

BY J. RIUS, J. SAÑE AND C. MIRAVITLLES

Institut de Ciència de Materials de Barcelona (CSIC), Campus de la UAB, 08193-Cerdanyola, Catalunya, Spain

AND H. GIES, B. MARLER AND U. OBERHAGEMANN

Institut für Mineralogie, Ruhr-Universität Bochum, D-44780 Bochum, Germany

(Received 17 December 1994; accepted 1 May 1995)

Abstract

The viability of solving the structure type of zeolitic and layered materials applying multisolution direct methods to low-resolution (~ 2.2 Å) powder diffraction data is shown. The phases are refined with the tangent formula derived from Patterson-function arguments [Rius (1993). *Acta Cryst.* **A49**, 406–409] and the correct phase sets are discriminated with the conventional figures of merit. The two test examples presented are (a) the already known tetragonal zeolite ZSM-11 (space group $I\bar{4}m2$) at 2.3 Å resolution and (b) the hitherto unknown layer silicate RUB-15 (*Ibam*) at 2.2 Å resolution. In both cases, the tetrahedral Si units appear as resolved peaks in the Fourier maps computed with the phases of the highest-ranked direct-methods solutions.

1. Introduction

To understand the physical and chemical properties of zeolitic and layered materials, and to retrieve valuable information about the synthesis mechanisms, a knowledge of their crystal structures is a prerequisite. When no sufficiently large single crystals are available, the crystal structure must be solved from very limited experimental data, such as powder diffraction, in combination with model building and other experimental techniques, *e.g.*

^{29}Si MAS NMR and electron diffraction. In recent years, the easier access to synchrotron X-ray sources, the existence of programs for extracting integrated intensities from high-resolution powder patterns (*e.g.* Pawley, 1981; Baerlocher, 1990) as well as improved computing facilities have rendered possible the *ab initio* solution of some highly crystalline zeolite-like compounds by direct methods (*e.g.* Rudolf, Saldarriaga-Molina & Clearfield, 1986; McCusker, 1988). The application of alternative methods, such as the direct interpretation of the Patterson function, is hampered by the relatively large number of tetrahedrally coordinated atoms (hereafter referred to as *T*) and by the fact that *T* atoms, *e.g.* Si, are not very much heavier than O atoms, so that the *T–T* interatomic peaks cannot be easily identified in the Patterson map. Other alternatives such as the application of Patterson search techniques, although viable (Rius & Miravittles, 1988; Gies & Rius, 1995), are far from trivial.

In many cases, zeolites crystallize as microcrystalline powders of poor crystallinity. The use of synchrotron radiation for these cases is less suitable. In these materials, peak broadening due to the sample often outweighs instrumental broadening so that only the low-resolution intensities can be extracted reliably from their powder patterns. This imposes serious limitations on the applicability of direct methods. These limitations have

been summarized in Sheldrick's empirical rule (Sheldrick, 1990) which states that it is very unlikely that the structure can be solved by direct methods if less than half the number of theoretically measurable reflections in the range $d = 1.1\text{--}1.2 \text{ \AA}$ are 'observed' [$F > 4\sigma(F)$]. This rule can be somewhat relaxed if heavy atoms are present. According to this rule, direct methods cannot be applied successfully to zeolites if only low-resolution intensity data ($d \geq 2.2 \text{ \AA}$) are available. In spite of this belief, and due to its practical interest, the possibility of solving zeolite-like materials from low-resolution data has been investigated. Should the solution be possible, then the structure type could be determined from laboratory powder data. The subsequent refinement using high-resolution intensity data, a step often requiring synchrotron radiation and/or the time-consuming optimization of the synthesis conditions, could be restricted to those compounds with favourable framework topology.

2. Theoretical background

According to their definition, the quasi-normalized structure factors are the structure factors of a structure consisting of point-like atoms. Conversely, a Fourier synthesis with these structure factors as coefficients should produce point-like atoms. In practice, however, only those intensities up to a given resolution $r_{\max}^* = 2 \sin \theta_{\max} / \lambda$ are accessible to the diffraction experiment. Consequently, the atomic peaks found in the Fourier map are not point like because of Fourier series-termination effects. Their shape, which depends on the r_{\max}^* value, is given by the Fourier transform

$$\begin{aligned} \eta(x) &= \int_{r^*=0}^{r_{\max}^*} 4\pi r^*{}^2 [\sin(2\pi x r^*) / 2\pi x r^*] dr^* \\ &= 4\pi [\sin(2\pi x r_{\max}^*) - 2\pi x r_{\max}^* \cos(2\pi x r_{\max}^*)] / (2\pi x)^3, \end{aligned} \quad (1)$$

where x is the distance to the atomic centre. The relationship between the position x_0 of the first zero of the $\eta(x)$ function and r_{\max}^* is given by

$$x_0 \simeq 0.72 / r_{\max}^*. \quad (2)$$

Expression (2) indicates that function $\eta(x)$ is sharp for large r_{\max}^* values and becomes broader for smaller r_{\max}^* values. Hence, neighbouring atomic peaks will overlap for small enough r_{\max}^* values.

As is well known, one of the basic requirements for direct methods to be successful is that the dominant scatterers are well resolved in the Fourier map. Only then are the phase values associated with the structure factors of the true and the squared structures similar. Of prime interest is the minimum r_{\max}^* value necessary for producing Fourier maps with the dominant scatterers well resolved. If the diffraction data do not reach this minimum value, it is improbable that direct methods can

solve the structure. Obviously, the minimum r_{\max}^* value will also depend on the closest separation between dominant scatterers. In organic structures, for example, the closest separation between C atoms is approximately 1.44 Å. To avoid peak overlap, x_0 cannot be greater than half this value, *i.e.* 0.72 Å. According to (2), this corresponds to $r_{\max}^* = 1 \text{ \AA}^{-1}$. This value agrees well with Sheldrick's empirical rule.

What happens in zeolite-like compounds? In such compounds, the closest separation between dominant scatterers (the Si atoms) is approximately 3.1 Å. The maximum allowed x_0 value is thus 1.55 Å, which corresponds to a r_{\max}^* value of 0.46 \AA^{-1} . This simple observation is of practical importance since it means that direct methods should solve zeolite-like structures using the intensities extracted from the low portion of the powder diffraction pattern ($r_{\max}^* = 0.46 \text{ \AA}^{-1}$ is equivalent to $2\theta = 41.5^\circ$ for Cu $K\alpha_1$ radiation). This portion is less affected by peak overlap problems so that, even with powder patterns measured on laboratory diffractometers, an almost complete intensity data set can be obtained. To simplify the above analysis, the presence of bridging O atoms, *i.e.* those that are common to two tetrahedra, has not been considered. Although the O atoms are weaker scatterers than the Si atoms, their presence could adversely affect the effectiveness of direct methods. As will be seen later in the test examples, this is not the case.

The above discussion suggests the viability of solving zeolite crystal structures by applying low-resolution multisolution direct methods. Owing to the small number of available intensities, however, the phase-refinement procedure must be very robust, *i.e.* it must actively use as many reflections as possible, it should avoid the introduction of complicated weighting schemes which can behave in an unstable way in such critical circumstances and, finally, it must be very effective. Since the tangent formula derived from Patterson-function arguments (Rius, 1993; Rius, Sañe, Miravittles, Amigó & Reventós, 1995) fulfils all these requirements, it has been selected for calculating the test examples. This tangent formula is implemented in the *XLENS* program (Rius, 1994).

3. Test examples

To test the tangent formula with low-resolution data, two representative examples have been selected. The first one is the already known tetragonal zeolite ZSM-11. This is a challenging example since ZSM-11 is a rather large zeolite with a symmorphic space group ($I4m2$). The second one is a previously unknown layer silicate with code name RUB-15.

3.1. The zeolite ZSM-11

ZSM-11 is a synthetic pentasil zeolite with a body-centred tetragonal cell. The structure was solved by

combining model building (Kokotailo, Chu, Lawton & Meier, 1978) and distance least-squares refinements (DLS; Meier & Villiger, 1969). Fig. 1 shows a perspective view of ZSM-11 along [010]. A detailed refinement of the structure was performed later with the intensity data of a powder sample collected at beam line X13A at Brookhaven National Laboratory ($\lambda = 1.3151 \text{ \AA}$, Ge(11) monochromator; Ge(220) analyzer; scanning interval $0.02^\circ/2\theta$; range $5\text{--}70^\circ/2\theta$; temperature 363 K ; capillary sample) (Pyle *et al.*, 1989). The refined lattice parameters (363 K) are $a = 20.067(1)$, $b = 13.411(1) \text{ \AA}$ and the found chemical composition per unit cell is $\text{Si}_{16}\text{O}_{40}$. The 87 integrated intensities for

Table 1. Positional parameters of the Si atoms for ZSM-11

(a) From Pyle *et al.* (1989). (b) From visual inspection of the Fourier map computed with the phases derived from low-resolution direct methods and shifting later the unit-cell origin by $1/2$ λ (average peak-position difference 0.98 \AA). The sites marked * are half-occupied to compensate for the increased multiplicity.

(a)		(b)	
x	y	x	y
Si(1)	0.078	0	0.062
Si(2)	0.186	0.21	0.055
Si(3)	0.186	0.21	0.055
Si(4)	0.230	0.312	0.040
Si(5)	0.195	0.02	0.062
Si(6)	0.194	0.12	0.139
Si(7)	0.076	0.320	0.076

combining model building (Kokotailo, Chu, Lawton & Meier, 1978) and distance least-squares refinements (DLS; Meier & Villiger, 1969). Fig. 1 shows a perspective view of ZSM-11 along [010]. A detailed refinement of the structure was performed later with the intensity data of a powder sample collected at beam line X13A at Brookhaven National Laboratory ($\lambda = 1.3151 \text{ \AA}$, Ge(11) monochromator; Ge(220) analyzer; scanning interval $0.02^\circ/2\theta$; range $5\text{--}70^\circ/2\theta$; temperature 363 K ; capillary sample) (Pyle *et al.*, 1989). The refined lattice parameters (363 K) are $a = 20.067(1)$, $b = 13.411(1) \text{ \AA}$ and the found chemical composition per unit cell is $\text{Si}_{16}\text{O}_{40}$. The 87 integrated intensities for

Table 1. Positional parameters of the Si atoms for ZSM-11

(a) From Pyle *et al.* (1989). (b) From visual inspection of the Fourier map computed with the phases derived from low-resolution direct methods and shifting later the unit-cell origin by $1/2$ λ (average peak-position difference 0.98 \AA). The sites marked * are half-occupied to compensate for the increased multiplicity.

(a)		(b)	
x	y	x	y
Si(1)	0.078	0	0.062
Si(2)	0.186	0.21	0.055
Si(3)	0.186	0.21	0.055
Si(4)	0.230	0.312	0.040
Si(5)	0.195	0.02	0.062
Si(6)	0.194	0.12	0.139
Si(7)	0.076	0.320	0.076

combining model building (Kokotailo, Chu, Lawton & Meier, 1978) and distance least-squares refinements (DLS; Meier & Villiger, 1969). Fig. 1 shows a perspective view of ZSM-11 along [010]. A detailed refinement of the structure was performed later with the intensity data of a powder sample collected at beam line X13A at Brookhaven National Laboratory ($\lambda = 1.3151 \text{ \AA}$, Ge(11) monochromator; Ge(220) analyzer; scanning interval $0.02^\circ/2\theta$; range $5\text{--}70^\circ/2\theta$; temperature 363 K ; capillary sample) (Pyle *et al.*, 1989). The refined lattice parameters (363 K) are $a = 20.067(1)$, $b = 13.411(1) \text{ \AA}$ and the found chemical composition per unit cell is $\text{Si}_{16}\text{O}_{40}$. The 87 integrated intensities for

Table 1. Positional parameters of the Si atoms for ZSM-11

(a) From Pyle *et al.* (1989). (b) From visual inspection of the Fourier map computed with the phases derived from low-resolution direct methods and shifting later the unit-cell origin by $1/2$ λ (average peak-position difference 0.98 \AA). The sites marked * are half-occupied to compensate for the increased multiplicity.

(a)		(b)	
x	y	x	y
Si(1)	0.078	0	0.062
Si(2)	0.186	0.21	0.055
Si(3)	0.186	0.21	0.055
Si(4)	0.230	0.312	0.040
Si(5)	0.195	0.02	0.062
Si(6)	0.194	0.12	0.139
Si(7)	0.076	0.320	0.076

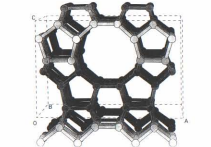


Fig. 1. ZSM-11. Perspective view along [010] of a portion of the tetragonal framework topology. Only the Si atoms are represented.

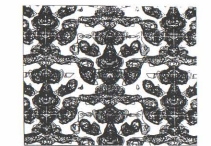


Fig. 2. ZSM-11. Superimposed Fourier sections ($y = 2/32$ to $14/32$) computed with the phases obtained applying direct methods to the lower portion of the synchrotron powder data ($D_{\text{max}} = 32.5^\circ$, $\lambda = 1.1515 \text{ \AA}$). The Si tetrahedra appear as isolated peaks. Their coordinates are listed in Table 1. To visualize the correspondence between found and refined peak positions, compare Figs. 1 and 2. The large broad peaks within the channels at $x = 0$ and $x = 1/2$ are spurious. The image was obtained with the program FAV (Vernonová & Linné, 1995).

the direct-methods test calculations were extracted from this preferred-orientation-free pattern ($D_{\text{max}} = 32.5^\circ$) with the program *AJUSZ*, a local program of *ICMAB* that fits Pearson VII profile functions. These intensities were introduced in *MLENS* with the overall B fixed at 5.5 \AA^2 and the phases of the 25 strongest F values refined (181 triplets of the $w \rightarrow s$ type ($s = \text{strong}$)). The program automatically selected the 20 weakest reflections for their active use during the phase refinement (291 triplets of the $w \rightarrow s$ type ($w = \text{weak}$); $E_{\text{th}} = 0.93$) (Rios *et al.*, 1995). The number of refined sets was 100 and the number of cycles was 15. Inspection of the Fourier map computed with the phase set possessing the best combined figure of merit (CFOM) indicates the existence of two types of peaks: the first constituted by peaks at approximately the correct positions (Table 1) and the second formed by strong incorrect maxima localized on the mirror planes $x = 0$ and $x = 1/2$ or, more specifically, in the centres of the channels of the structure. Fig. 2 is the image obtained by superposition of the Fourier sections from $y = 2/32$ to $14/32$. The peaks in Fig. 2 can be easily identified, comparing Figs. 1 and 2.

3.2. The layered material RUB-15

In view of the promising results achieved with ZSM-11, the same strategy was applied to the determination of the structure of RUB-15. The powder diffraction pattern was measured on a Siemens diffractometer at the Ruhr University (Bochum) ($\lambda = 1.54060 \text{ \AA}$, Ge(11) monochromator; scanning interval $0.02^\circ/2\theta$; counting time 30 s ; range $5\text{--}70^\circ/2\theta$; temperature 293 K ; capillary sample). The powder pattern was indexed on an orthorhombic unit cell with $a = 27.911$, $b = 8.408$, $c = 11.516 \text{ \AA}$, $V = 2703 \text{ \AA}^3$ using the program *TREOR* (Werner, Erikson & Wondratsch, 1985). According to the systematic absences, the cell is body centred and the most likely space group is *I*2mm. With all the prior experimental information about the compound taken into account, the expected numbers of Si atoms and template molecules in the unit cell are approximately 28 and 8, respectively.

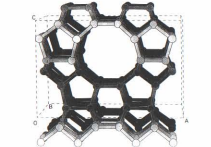


Fig. 1. ZSM-11. Perspective view along [010] of a portion of the tetragonal framework topology. Only the Si atoms are represented.

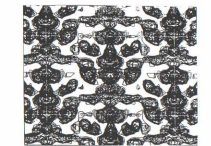


Fig. 2. ZSM-11. Superimposed Fourier sections ($y = 2/32$ to $14/32$) computed with the phases obtained applying direct methods to the lower portion of the synchrotron powder data ($D_{\text{max}} = 32.5^\circ$, $\lambda = 1.1515 \text{ \AA}$). The Si tetrahedra appear as isolated peaks. Their coordinates are listed in Table 1. To visualize the correspondence between found and refined peak positions, compare Figs. 1 and 2. The large broad peaks within the channels at $x = 0$ and $x = 1/2$ are spurious. The image was obtained with the program FAV (Vernonová & Linné, 1995).

the direct-methods test calculations were extracted from this preferred-orientation-free pattern ($D_{\text{max}} = 32.5^\circ$) with the program *AJUSZ*, a local program of *ICMAB* that fits Pearson VII profile functions. These intensities were introduced in *MLENS* with the overall B fixed at 5.5 \AA^2 and the phases of the 25 strongest F values refined (181 triplets of the $w \rightarrow s$ type ($s = \text{strong}$)). The program automatically selected the 20 weakest reflections for their active use during the phase refinement (291 triplets of the $w \rightarrow s$ type ($w = \text{weak}$); $E_{\text{th}} = 0.93$) (Rios *et al.*, 1995). The number of refined sets was 100 and the number of cycles was 15. Inspection of the Fourier map computed with the phase set possessing the best combined figure of merit (CFOM) indicates the existence of two types of peaks: the first constituted by peaks at approximately the correct positions (Table 1) and the second formed by strong incorrect maxima localized on the mirror planes $x = 0$ and $x = 1/2$ or, more specifically, in the centres of the channels of the structure. Fig. 2 is the image obtained by superposition of the Fourier sections from $y = 2/32$ to $14/32$. The peaks in Fig. 2 can be easily identified, comparing Figs. 1 and 2.

3.2. The layered material RUB-15

In view of the promising results achieved with ZSM-11, the same strategy was applied to the determination of the structure of RUB-15. The powder diffraction pattern was measured on a Siemens diffractometer at the Ruhr University (Bochum) ($\lambda = 1.54060 \text{ \AA}$, Ge(11) monochromator; scanning interval $0.02^\circ/2\theta$; counting time 30 s ; range $5\text{--}70^\circ/2\theta$; temperature 293 K ; capillary sample). The powder pattern was indexed on an orthorhombic unit cell with $a = 27.911$, $b = 8.408$, $c = 11.516 \text{ \AA}$, $V = 2703 \text{ \AA}^3$ using the program *TREOR* (Werner, Erikson & Wondratsch, 1985). According to the systematic absences, the cell is body centred and the most likely space group is *I*2mm. With all the prior experimental information about the compound taken into account, the expected numbers of Si atoms and template molecules in the unit cell are approximately 28 and 8, respectively.

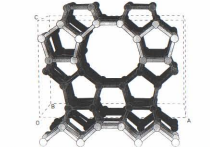


Fig. 1. ZSM-11. Perspective view along [010] of a portion of the tetragonal framework topology. Only the Si atoms are represented.

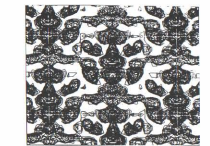


Fig. 2. ZSM-11. Superimposed Fourier sections ($y = 2/32$ to $14/32$) computed with the phases obtained applying direct methods to the lower portion of the synchrotron powder data ($D_{\text{max}} = 32.5^\circ$, $\lambda = 1.1515 \text{ \AA}$). The Si tetrahedra appear as isolated peaks. Their coordinates are listed in Table 1. To visualize the correspondence between found and refined peak positions, compare Figs. 1 and 2. The large broad peaks within the channels at $x = 0$ and $x = 1/2$ are spurious. The image was obtained with the program FAV (Vernonová & Linné, 1995).

the direct-methods test calculations were extracted from this preferred-orientation-free pattern ($D_{\text{max}} = 32.5^\circ$) with the program *AJUSZ*, a local program of *ICMAB* that fits Pearson VII profile functions. These intensities were introduced in *MLENS* with the overall B fixed at 5.5 \AA^2 and the phases of the 25 strongest F values refined (181 triplets of the $w \rightarrow s$ type ($s = \text{strong}$)). The program automatically selected the 20 weakest reflections for their active use during the phase refinement (291 triplets of the $w \rightarrow s$ type ($w = \text{weak}$); $E_{\text{th}} = 0.93$) (Rios *et al.*, 1995). The number of refined sets was 100 and the number of cycles was 15. Inspection of the Fourier map computed with the phase set possessing the best combined figure of merit (CFOM) indicates the existence of two types of peaks: the first constituted by peaks at approximately the correct positions (Table 1) and the second formed by strong incorrect maxima localized on the mirror planes $x = 0$ and $x = 1/2$ or, more specifically, in the centres of the channels of the structure. Fig. 2 is the image obtained by superposition of the Fourier sections from $y = 2/32$ to $14/32$. The peaks in Fig. 2 can be easily identified, comparing Figs. 1 and 2.

3.2. The layered material RUB-15

In view of the promising results achieved with ZSM-11, the same strategy was applied to the determination of the structure of RUB-15. The powder diffraction pattern was measured on a Siemens diffractometer at the Ruhr University (Bochum) ($\lambda = 1.54060 \text{ \AA}$, Ge(11) monochromator; scanning interval $0.02^\circ/2\theta$; counting time 30 s ; range $5\text{--}70^\circ/2\theta$; temperature 293 K ; capillary sample). The powder pattern was indexed on an orthorhombic unit cell with $a = 27.911$, $b = 8.408$, $c = 11.516 \text{ \AA}$, $V = 2703 \text{ \AA}^3$ using the program *TREOR* (Werner, Erikson & Wondratsch, 1985). According to the systematic absences, the cell is body centred and the most likely space group is *I*2mm. With all the prior experimental information about the compound taken into account, the expected numbers of Si atoms and template molecules in the unit cell are approximately 28 and 8, respectively.

The integrated intensities were extracted with *EXTRACT* (Baerlocher, 1990) using an experimental peak-shape function ($\text{FWHM} = 0.08^\circ 2\theta$). Above $2\theta = 41^\circ$, most of the integrated intensities supplied by *EXTRACT* have associated standard deviations that are too large. Consequently, they were not considered. The 76 low-resolution reflections were introduced in *XLENS* with the overall B fixed at 3.5 \AA^2 . The program was selected to refine the phases of the 20 strongest E values (65 triplets of the s - s - s type). The program automatically selected the 16 weakest reflections for their active use during the phase refinement (98 triplets of the w - s - s type; $\langle E_H \rangle = 1.0$) (Rius *et al.*, 1995). The number of refined sets was 100 and the number of calculated cycles in each set was 13. The projection of the Fourier map for the solution with the highest CFOM is shown in Fig. 3. It can be clearly seen that the structure consists of silicate sheets (a perspective view of one sheet is given in Fig. 4) and that the Si tetrahedra appear as resolved spheres (Table 2). The relative strength of the O atoms can be estimated by comparing one of these spheres with the spheres representing the non-bridging or terminal O atoms of the sheet. Inspection of Fig. 3 also allows one to distinguish quite clearly, between the sheets, the tetrahedral tetramethylammonium molecules positioned on the mirror planes. The nature of the remaining peaks is less clear (Table 2). The subsequent Rietveld refinement has revealed that O(1) is a tetrahedrally coordinated water molecule, and that Q1 and Q2 are spurious peaks. Fig. 5 reproduces the observed and the calculated powder diffraction patterns (present R_{wp} value 17%).

To check the reproducibility of the direct-methods results, the phase-refinement control parameters were

Table 2. Peaks found in the Fourier map of the direct-methods solution with the highest combined figure of merit for RUB-15

Only the low-resolution intensities extracted from a laboratory powder pattern have been used ($2\theta_{\text{max}} = 41^\circ$; $\text{Cu K}\alpha_1$ radiation).

	Site	x	y	z	
	Si(1)	16(k)	0.056	0.250	0.381
	Si(2)	4(b)	0	1/2	1/4
	Si(3)	4(a)	0	0	1/4
	N	8(j)	0.146	0.292	0
	O(1)	16(k)	0.300	0.291	0.118
	Q1	8(j)	0.250	0.458	0
	Q2	8(e)	1/4	1/4	1/4

slightly changed. Inspection of the best sets of refined phases again showed the same solution.

4. Concluding remarks

The above results can be summarized in the following conclusions:

(a) In principle, it is possible to determine the connectivity pattern of tetrahedral frameworks and sheets applying multisolution direct methods to low-resolution intensity data. The lowest resolution limit is $r_{\text{max}}^* \approx 0.46 \text{ \AA}^{-1}$, *i.e.* all reflections with d spacings greater than 2.2 \AA are required. At this resolution, the tetrahedral Si units appear as well resolved peaks in the Fourier map. Obviously, the higher the resolution limit of the data, the better direct methods will work. One difficulty that can arise when only low-resolution data are available is the correct estimation of the space group.

(b) The tangent formula derived from Patterson-function argument (Rius, 1993) is well suited for phase

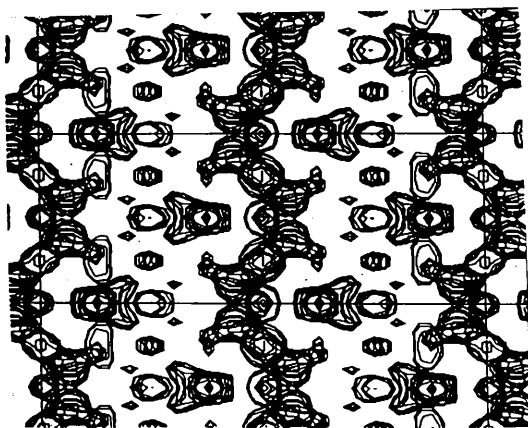


Fig. 3. RUB-15. Superimposed Fourier sections ($y = 0$ to 0.45) showing the silicate sheets normal to $[100]$. The phases were obtained from low-resolution direct methods ($d \geq 2.2 \text{ \AA}$). At this resolution, the tetrahedral Si units appear as spheres. The tetramethylammonium molecules are placed on the mirror planes. The peak coordinates are listed in Table 2. Image obtained with *FAN* (Vernoslova & Lunin, 1993).

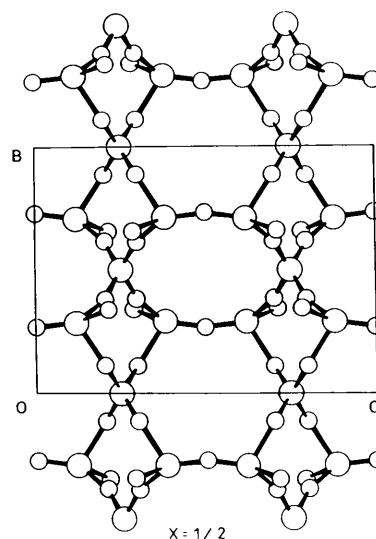


Fig. 4. RUB-15. Silicate sheet built of four- and six-membered rings in the ratio 1:1 (large circles: Si atoms; small circles: O atoms).

refinement with low-resolution intensity data. The appearance of large incorrect maxima concentrated on the non-translational symmetry elements in the Fourier map of ZSM-11 is surely related to the fact that $I\bar{4}m2$ is symmorphic. This effect may be favoured by the small number of reflections involved in the phase refinement and/or by pseudosymmetry problems, relevant to this

compound, and requires further investigation. In ZSM-11, these incorrect peaks can be easily identified so that the interpretation of the remaining peaks, *i.e.* the Si units, is not greatly disturbed.

(c) The traditional figures of merit work well. In both test examples, the solutions with the highest CFOM are the correct ones.

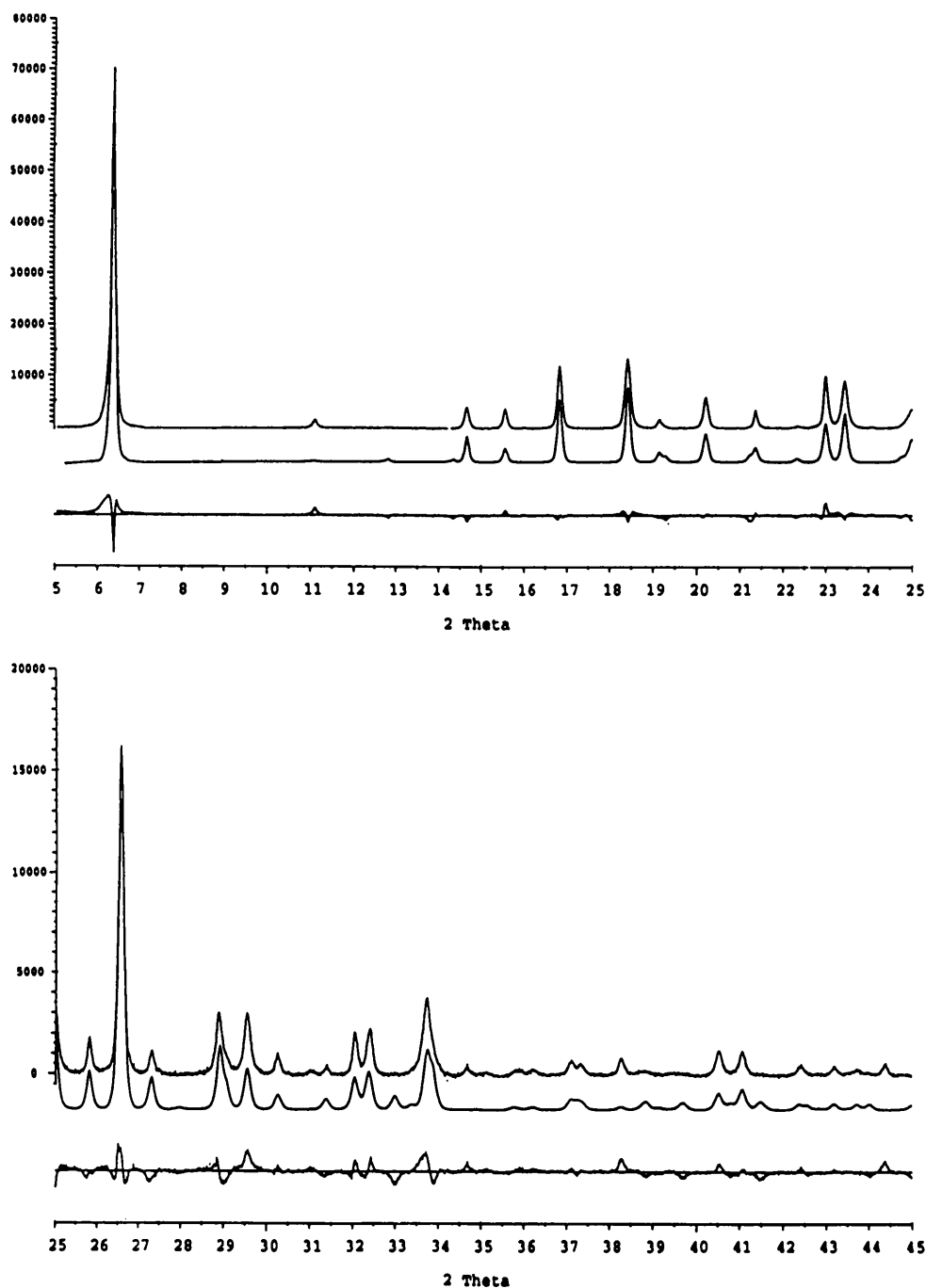


Fig. 5. RUB-15. Observed (top), calculated (middle) and difference (bottom) profiles for the provisional Rietveld refinement. To facilitate comparison, the scale for the interval 25–45° has been increased by a factor of four.

(d) The Fourier maps must be visually inspected. Automated peak search routines can often produce misleading results. Although low-resolution data are very sensitive to the presence of atomic peaks, these can appear slightly shifted from the correct position. This is especially true for structures possessing non-centrosymmetric space groups. Effectively, since general reflections have no restricted phase values, small phase errors associated with the direct-methods application cannot be eliminated, thus producing inaccuracies in the atomic positioning in the *E* map. For these space groups, average atomic displacements of the order of 0.5 Å should be considered normal.

This work was supported by the Spanish DGICYT (Project PB92-010) and the acción integrada hispano-alemana HA94-086. The authors are greatly indebted to Drs E. A. Vernoslova and V. Yu. Lunin, as well as to Dr A. Urzhumtsev for kindly supplying the *Frog* PC series programs.

Acta Cryst. (1995). **A51**, 845–849

Simulated Annealing as a Tool for *Ab Initio* Phasing in X-ray Crystallography

BY WU-PEI SU

Department of Physics and Texas Center for Superconductivity, University of Houston, Houston, Texas 77204, USA

(Received 23 January 1995; accepted 9 June 1995)

Abstract

Simulated annealing has traditionally been used to refine structural determinations. It is shown in this paper that it can be used for *ab initio* phasing. Several examples are given to illustrate the methodology and capability of this method. The possibility of extending the method to treat macromolecules is discussed.

Introduction

Traditional direct methods are based on the probability distribution of the phases of the structure factors given their magnitudes. The width of the distribution increases with the number of atoms *N* in the unit cell. Therefore, the method is not practical for large *N* (Hauptman, 1986) but there are many interesting large molecules whose structures remain to be resolved. Thus, it is very desirable to explore alternate methods for *ab initio* phasing. Semenovskaya, Khachatryan & Khachatryan (1985) have proposed a statistical mechanics approach. They employed stochastic dynamic equations to generate atom positions that optimally fit the measured intensities. In essence, this is a dynamical simulated-

References

- BAERLOCHER, C. (1990). *EXTRACT. A Fortran Program for the Extraction of Integrated Intensities from a Powder Pattern*. Institut für Kristallographie, ETH, Zürich, Switzerland.
- FYFE, C. A., GIES, H., KOKOTAILO, G. T., PASZTOR, C., STROBL, H. & COX, D. E. (1989). *J. Am. Chem. Soc.* **111**, 2470–2474.
- GIES, H. & RIUS, J. (1995). *Z. Kristallogr.* In the press.
- KOKOTAILO, G. T., CHU, P., LAWTON, S. L. & MEIER, W. M. (1978). *Nature (London)*, **275**, 119.
- MCCUSKER, L. B. (1988). *J. Appl. Cryst.* **21**, 305–310.
- MEIER, W. M. & VILLIGER, H. Z. (1969). *Z. Kristallogr.* **129**, 411.
- PAWLEY, G. S. (1981). *J. Appl. Cryst.* **14**, 357–361.
- RIUS, J. (1993). *Acta Cryst.* **A49**, 406–409.
- RIUS, J. (1994). *XLENS. A Program for Crystal Structure Determination*. ICMAB-CSIC, Catalunya, Spain.
- RIUS, J. & MIRAVITLLES, C. (1988). *J. Appl. Cryst.* **21**, 224–227.
- RIUS, J., SAÑÉ, J., MIRAVITLLES, C., AMIGÓ, J. M. & REVENTÓS, M. M. (1995). *Acta Cryst.* **A50**, 268–270.
- RUDOLF, P. R., SILDARRIAGA-MOLINA, C. & CLEARFIELD, A. (1986). *J. Phys. Chem.* **90**, 6122–6125.
- SHELDRIK, G. M. (1990). *Acta Cryst.* **A46**, 467–473.
- VERNOSLOVA, E. A. & LUNIN, V. YU. (1993). *J. Appl. Cryst.* **26**, 291–294.
- WERNER, P.-E., ERIKSON, L. & WESTDAHL, M. (1985). *J. Appl. Cryst.* **18**, 367–370.

annealing approach. They applied this approach to a unit cell containing eight independent atoms. In this paper, we report more extensive calculations of direct structural determination using simulated annealing. Our results suggest that this method is a promising alternate to conventional direct methods. More importantly, it is very straightforward to incorporate symmetry and other partial knowledge about the molecules in this scheme. Thus, it is potentially possible to extend the method to treat macromolecules such as proteins.

This paper is organized as follows: We first discuss the methodology in general. The three molecules on which the method has been successfully tested are then described. Test results on a new system that has not been solved by direct methods are also reported. Based on these results, comparison with conventional direct methods and some alternate methods is made. Finally, we speculate on the possibility of applying the formalism to protein crystallography.

Methodology

The idea of a simulated-annealing approach to the X-ray phase problem is very simple. Basically, the method con-